An optimal design for the injection and extraction elements for the RIKEN Superconducting Ring Cyclotron

T. Tominaka, H. Okuno, S. Fujishima, A. Goto, and Y. Yano

The Institute of Physical and Chemical Research (RIKEN), 2-1, Hirosawa, Wako, Saitama, 351-0106, Japan

The injection and extraction systems for a 6-sector Superconducting Ring Cyclotron (SRC) of the RIKEN RI Beam Factory project consists of bending magnets, magnetic inflection and deflection channels and electrostatic inflection and deflection channels. Especially, several bending magnets and magnetic channels are superconducting. An active-shield type magnet which is equipped with a pair of shield coils is adopted for these dipole magnets. In this article, optimization of the cross-sectional shape of an active-shield type dipole magnet is described.

1 Introduction

The beam trajectories and whole layout of the injection and extraction systems for SRC are under study.[1, 2] The superconducting dipole magnets for these systems are planned to be an active-shield type, as shown in Fig. 1, due to the fringe field of the sector magnets.

2 Optimization Method

The superconducting dipole magnets are planned to be composed of rectangular current-carrying current blocks to ease the coil fabrication.[3] Major parameters of MIC3 are listed in Table 1. A procedure to optimize the cross sectional shape is studied here with the following two steps:[4]

1) Rough optimization of the size and location of the current-carrying blocks.

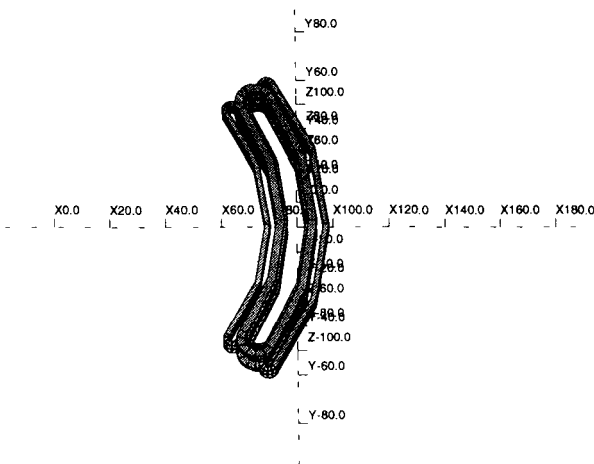2) Precise optimization of the locations of rectangular current blocks.

As the first step of optimization, a linear programming (LP) method can be used to acquire the initial cross sectional shape for further optimization in the second step. In general, LP is effective to find the global minimum or maximum of any linear function subject to a set of constraints defined by linear inequalities. On the other hand, as the second step, an optimization method to find the local minima of arbitrary function is adopted. Then, the global minimum of this optimization problem is found by the combination of these two steps.

Table 1 : Major parameters of MIC3.

Bending field	1.5 T
Bore size	$40mm(H) \times 30mm(V)$
2D Homogeneity	1×10^{-3}
Bending radius	0.87 m
Effective magnetic angle	73.9 deg.
Stray field	$< 100G$ at $0.25m$

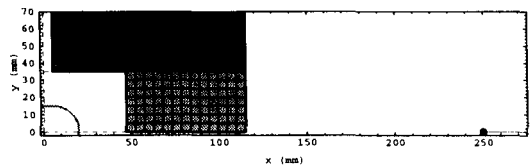Figure 1: Schematic view of the active-shield type dipole magnet.

Figure 2: Cross section of a magnetic inflection channel of the active shield type (MIC3), with the conductor (shaded) region for a linear programming.

A quarter of the cross-sectional geometry for optimization is shown in Fig. 2. The region permitted as the location for current-carrying blocks is divided into small rectangular elements. The upper darker elements are reserved only for the main coil, while the lower elements are for both main and shield coils, constrained from the requirement of the final coil configuration. The

current in each element is optimized by LP in such a way that the field homogeneity within the racetrack boundary $(40mm(H) \times 30mm(V))$, shown by the gray line in Fig. 2, is better than 0.1 %, and the fringe field at $x > 0.25m$ on the horizontal axis, shown by a bullet in Fig. 2, is below 100 G. In this LP, the following objective function and various constraints are expressed by linear function and inequalities,

- objective function : total ampere turn,
- constraint (1) : minimum central field,
- constraint (2) : maximum current density,
- constraint (3) : lowest field homogeneity,
- constraint (4) : maximum fringe field,
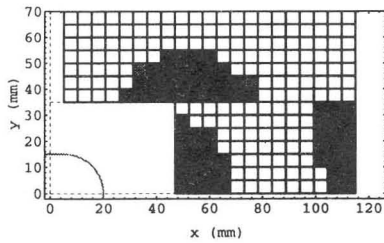- constraint (5) : maximum difference of currents between the lower main and shield blocks.

Figure 3: Optimal cross section obtained by LP .

As a result of LP, the current of each element is obtained, as shown with the darker element for the higher current in Fig. 3. Then, it is realized that the optimized current distribution is approximated by two main rectangular current blocks and one shield current block, as shown in Fig. 4. However, this conversion to the rectangular shape of current block induces a deviation from the optimized arrangement in step 1.
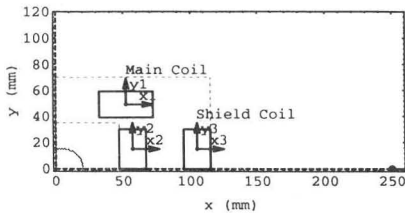

Figure 4: Cross section of a magnetic inflection channel of active shield type (MIC3) (the second optimization).

As the second step which is a cross sectional position optimization step, the horizontal and vertical positions of each current block shown as (x_1, y_1), (x_2, y_2), and (x_3, y_3) in Fig. 4, corresponding to the coordinates in Figs. 5 and 6 are optimized. The procedure of the second step is as follows: [5, 6]

1) Calculation of the interior and exterior multipoles

determined from the cross sectional configuration of coil.

2) Calculation of the field homogeneity from the interior multipoles and of the fringe field from the exterior multipoles.

3) Search for the optimal locations of each current block to maximize the field homogeneity with the constraint for the fringe field.

The relation between the field homogeneity and the interior multipoles of dipole coils, and that between the fringe field and the exterior multipoles can be geometrically obtained for the specific homogeneous regions like the racetrack and for the requirement of the fringe field. [6] Then, these relations are used for the calculation of the field homogeneity and of the fringe field.

The optimal locations of each current block corresponding to the minimum value of the fraction to maximize the field homogeneity and the allowable fringe field can be sought as the overlapped region of the two contour plots, as shown in Figs. 5 and 6.
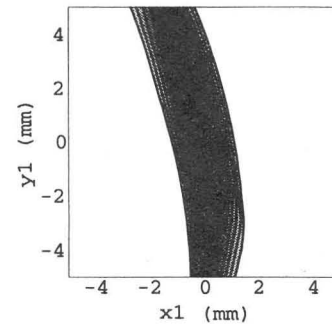

Figure 5: Contour plot of (x_1, y_1) plane, satisfying $|(B_y - B_{y0})/(B_{y0} + 4)| < 0.1\%$, with $x_2, y_2, x_3, y_3 = 0$.
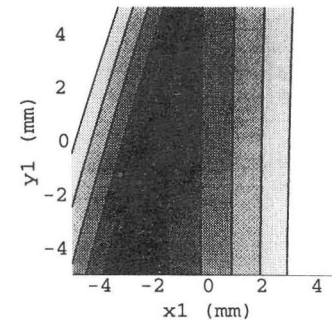

Figure 6: Contour plot of (x_1, y_1) plane, satisfying $|B_y(x > 0.25m)| < 100G$, with $x_2, y_2, x_3, y_3 = 0$.

In these figures, the darker region corresponds to the favorable homogeneity (smaller value of the fraction) or

the minimum fringe field, while the white region is out of the requirement.

As a result, the optimal coil configuration producing the interior field distribution shown by Fig. 7, and the exterior field distribution shown by Fig. 8, can be obtained with the satisfaction of requirements by this optimization method.
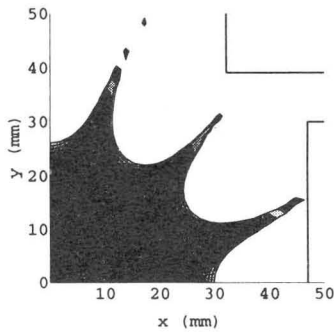

Figure 7: Homogeneous field region, satisfying $|(B_y - B_{y0})/(B_{y0} + 4)| < 0.1\%$ (2D calculation).
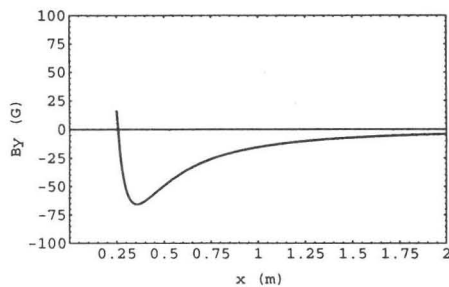

Figure 8: Distribution of the fringe field, B_y, on the x axis ($x > 0.25m$) (2D calculation).

3   Field Analysis

3.1   2D Calculation

For the case with the vertical bias field of $B_{bias} = +4.0T$ due to the sector magnet, The 2D field analysis for the MIC3 is made analytically, using the Biot-Savart law. The distribution of field vectors is shown in Fig. 9, together with the cross section of current blocks. The vertical bias field B_{bias} decreases the total field between the main and shield current blocks, and changes the magnetic forces acting on each current blocks. The contour plot of $|B|$ is also shown in Fig.10. The maximum field of coils is about 6.0 T similarly with that at the center of 3D calculation.
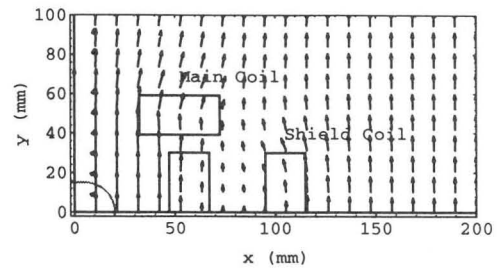

Figure 9: Field distribution with the bias field of 4 T and cross section for magnetic inflection channel of the active shield type.
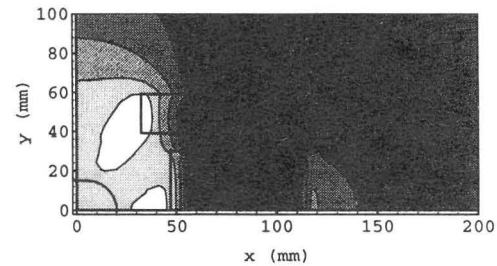

Figure 10: Contour plot of $|B|$ on the case with the bias field of 4 T due to the sector magnet.

3.2   3D Calculation

The 3D field analysis for the MIC3 is made mainly for the field calculation at the coil end, using the program of OPERA-3d. [7] The schematic view of a half of MIC3 consisting the coil head with spacers is shown in Fig. 11. The contour plot of $|B|$ at the center of the curved body and the boundary between the body and end part (shown as two dashed lines in Fig. 11) are also shown in Figs. 12 and 13. The highest field of coils is about 6.3 T near the boundary between the body and end part even with the spacers in coil ends. The fringe field for the nearest first equilibrium orbit as a parameter of the angle at the center of the coil curvature is also shown in Fig. 14. In addition, the calculated multipoles for the reference radius, $r_0 = 20mm$, like dipole, quadrupole, etc., are shown in Figs. 15 to 17. The coil end shown in Fig. 11 is not optimal for the integrated multipoles along the beam axis. Then, optimization for the shape of the end is still under study at present.

4   Conclusion

It is realized that this 2D optimization is enough for the search of the optimal cross section except the coil end, from the comparison between 2D and 3D field analysis. In addition, this optimization with 2 step will be useful to optimize the cross-sectional shape of dipole coils such
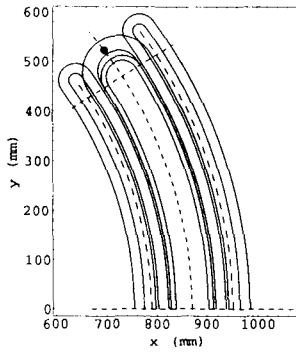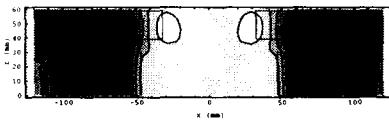
Figure 11: Schematic top view of MIC3.

Figure 12: Contour plot of $|B|$ on the case with the bias field (at the boundary between the curved body and end parts).

as the injection and extraction bending magnets of the SRC.

References

[1] S. Fujishima et al., in this proceedings.

[2] H. Okuno et al., in this proceedings.

[3] C. R. Hoffmann et al., *Proc. 10th Int. Conf. on Cyclotron and their Appli.*, pp.222 - 225 (1984).

[4] M. Kitamura et al., *IEEE Trans.* MAG-30 pp.2352 - 2355 (1994).

[5] T. Tominaka et al., *Proc. of 1997 Particle Accelerator Conference*, to be published.

[6] T. Tominaka et al., *Proc. of 15-th Magnet Technology Conference*, (1997); to be published.
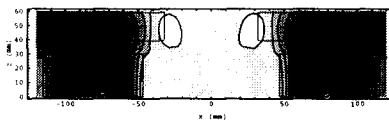
[7] Vector Field Limited, Oxford, England.

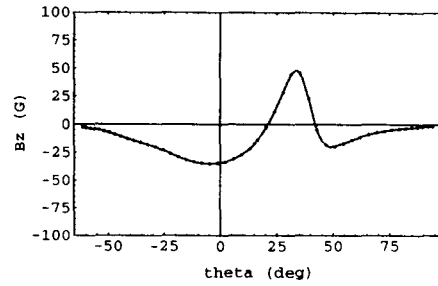Figure 13: Contour plot of $|B|$ on the case with the bias field (at the center).

Figure 14: B_z along the first equilibrium orbit of $^{238}U^{58+}$ near MIC3.
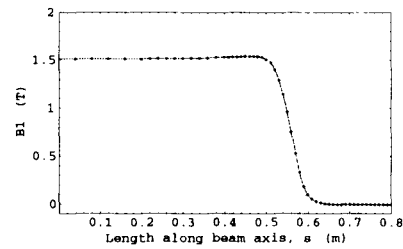
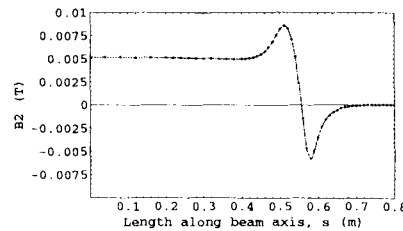Figure 15: Dipole vs the distance from the center along the beam axis.

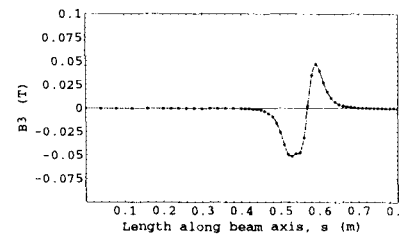Figure 16: Quadrupole vs the distance from the center along the beam axis.

Figure 17: Sextupole vs the distance from the center along the beam axis.